

# From Point Defects in Graphene to Two-Dimensional Amorphous Carbon (Supplementary information)

J. Kotakoski<sup>1</sup>, A. V. Krasheninnikov<sup>1,2</sup>, U. Kaiser<sup>3</sup> and J. C. Meyer<sup>3</sup>

<sup>1</sup> *Department of Physics, University of Helsinki,  
P.O. Box 43, 00014 Helsinki, Finland*

<sup>2</sup> *Department of Applied Physics, Aalto University,  
P.O. Box 1100, 00076 Aalto, Finland*

<sup>3</sup> *Electron microscopy of materials science, University of Ulm, Germany*

## Methods

As described in the main article, graphene membranes were prepared by micro-mechanical cleavage and transfer to TEM grids [1]. Aberration-corrected HRTEM imaging was carried out in an FEI Titan 80–300, equipped with an objective-side image corrector. The microscope was operated at 80 keV and 100 keV for HRTEM imaging, and at 300 keV for irradiation. The extraction voltage of the field emission source was set to a reduced value of 2 kV in order to reduce the energy spread. For both 80 keV and 100 keV imaging, the spherical aberration was set to  $20 \text{ \AA}\mu\text{m}$  and images were obtained at Scherzer defocus (ca.  $-9 \text{ nm}$ ). At these conditions, dark contrast can be directly interpreted in terms of the atomic structure. Image sequences were recorded on the CCD camera with exposure times ranging from 1 s to 3 s and intervals between 4 s and 8 s, and a pixel size of  $0.2 \text{ \AA}$ . The effect of slightly uneven illumination is removed by normalization (division) of the image to a strongly blurred copy of the same image, effectively removing long-range variations. Drift-compensation is done using the Stackreg plugin for the ImageJ software [2]. We show individual exposures as well as averages of a few frames (up to 10). This is because we have used different beam current densities, in order to test for possible dose rate effects (within the 100 keV, simultaneous imaging and defect generation experiment). The configurations described here can be discerned in individual exposures if ca.  $10^4$  counts per pixel at  $0.2 \text{ \AA}$  pixel size are used. With a high beam current density, this is possible in 1 s exposures (corresponding to a total dose of ca.  $10^5 \frac{e^-}{\text{\AA}^2}$  per image, and a dose rate of  $10^5 \frac{e^-}{\text{\AA}^2 \cdot \text{s}}$ ). At lower current densities, the same dose was spread over several exposures, so that sample drift could be compensated (individual exposures could not be longer than 3 s due to sample drift). The lowest dose rate was ca.  $3 \cdot 10^3 \frac{e^-}{\text{\AA}^2 \cdot \text{s}}$ . Within our dose rate range, density and shape of defects appears to depend only on the total dose.

Formation energy of a structure in our DFT calculations was defined in the usual way as

$$E_f(V_n) = E_{\text{tot}}(V_n) - E_{\text{tot}}^{\text{gr}} + n\mu_{\text{gr}}, \quad (1)$$

where  $E_{\text{tot}}(V_n)$  and  $E_{\text{tot}}^{\text{gr}}$  are the total energies of the structure with the defect ( $n$  missing atoms) and the same supercell without the defect, respectively, and  $\mu_{\text{gr}}$  is the chemical potential of a carbon atom in pristine graphene. The semi-conducting features of the defects were consistently observed with varying number of  $k$ -kpoints used in calculating the electronic density of states.

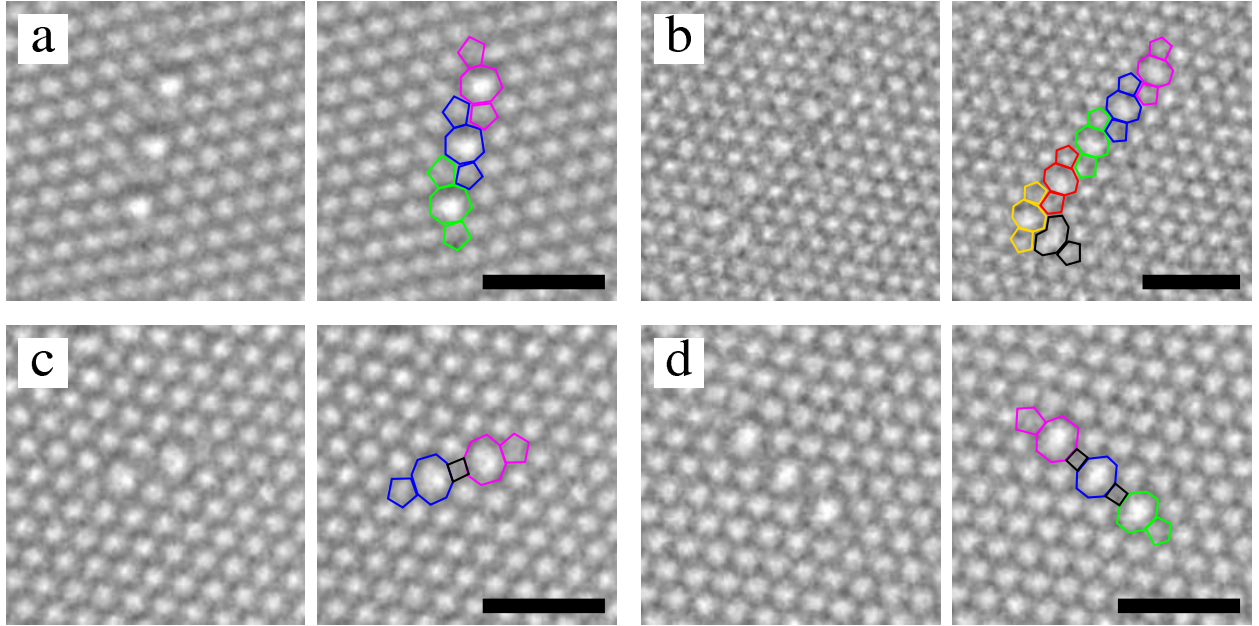


Figure 1: Images of di-vacancy (DV) defects in linear alignment, shown with and without structure overlay in each case. (a) Three DVs aligned along the zigzag direction of the graphene lattice. (b) Five DVs aligned in zigzag direction, clustered with a single vacancy (black). (c) Two DVs aligned along the armchair direction, forming a carbon tetragon at their intersection. (d) Three DVs aligned along the armchair direction, forming two carbon tetragons. All scale bars are 1 nm.

### Further images

For clarity we show here the TEM images of the main article without structure overlay, and also a few additional TEM images. Fig. 1 shows several di-vacancy (DV) defects in linear alignment. In particular, the carbon tetragon is always reproduced when the DVs are aligned along the armchair direction of the graphene lattice. Fig. 2 shows a comparison between a HRTEM image simulation based on a DFT-optimized structure and an actual HRTEM image for the armchair alignment of di-vacancies.

In Fig. 3, we show the panels a–d from the Figure 3 of the main article with and without overlays. These images are also contained in Supplementary video S2. In Fig. 4 we show panels a–h from the Figure 4 of the main article with and without overlay (the corresponding time series is shown in Supplementary video S3).

In Fig. 5, we show two additional images where a defect with a rotated hexagon kernel was generated from clusters of multiple vacancies. These configurations were created by



Figure 2: DFT-optimized structure of the defect with two tetragons (a), HRTEM simulation based on the DFT-structure (b) and the HRTEM image of the same structure for comparison (c). Scale bar is 1 nm.

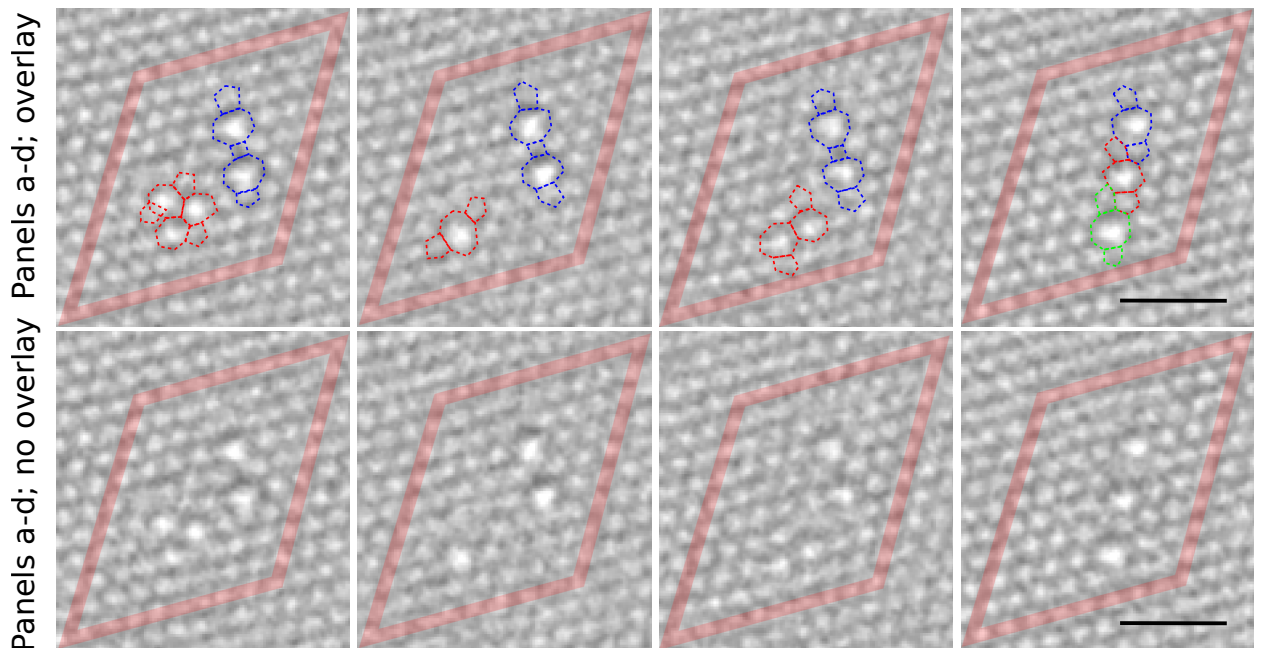


Figure 3: Panels a-d from Figure 3 of the main article with and without overlays. Scale bar is 1 nm.

a short 300 keV exposure and subsequent imaging at 80 keV. It should be noted that the rotated hexagon kernels appear in the larger vacancy clusters in both of our experiments (100 keV irradiation with simultaneous imaging as in Figure 4 of the main article, and the 300 keV/80 keV combination as shown in Fig. 5).

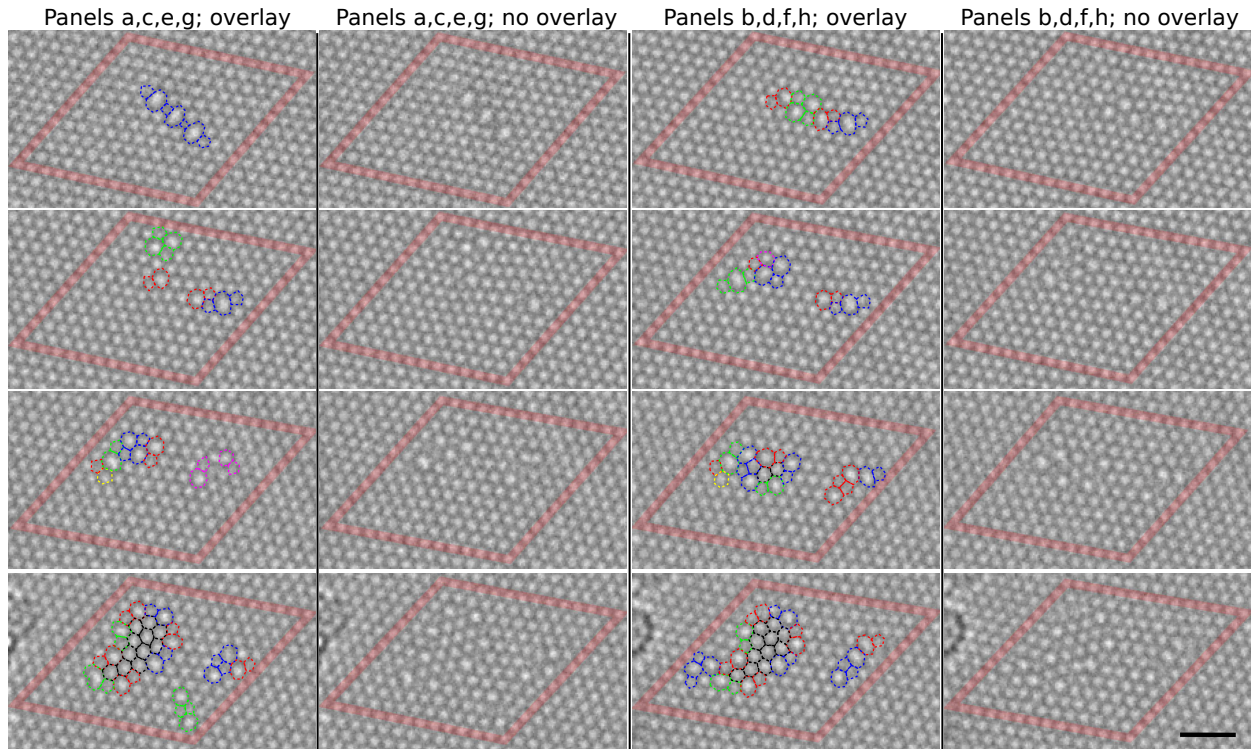


Figure 4: Panels a–h from Figure 4 of the main article with and without overlays. Scale bar is 1 nm.

### Description of the supplementary videos

*Supplementary video S1:* Generation and transformation of defects under 100 keV irradiation. Each frame is an average of 2 CCD exposures. Note the continuous increase in defect density and partial amorphization of the membrane.

*Supplementary video S2:* Further transformation of graphene to a 2D amorphous membrane under 100 keV irradiation. In terms of total dose, it can be considered as a continuation of video S4 (although sample region is different). Each frame shows an individual CCD exposure. Note that the entire clean graphene area becomes amorphous while remaining one-atom thick, and beam-generated holes make up only a small fraction of the area.

*Supplementary video S3:* Two isolated di-vacancies, generated by brief 300 keV irradiation and observed at 80 keV. The di-vacancies migrate under the beam and transform between the  $V_2(5-8-5)$ ,  $V_2(555-777)$  and  $V_2(5555-6-7777)$  configurations multiple times. The video

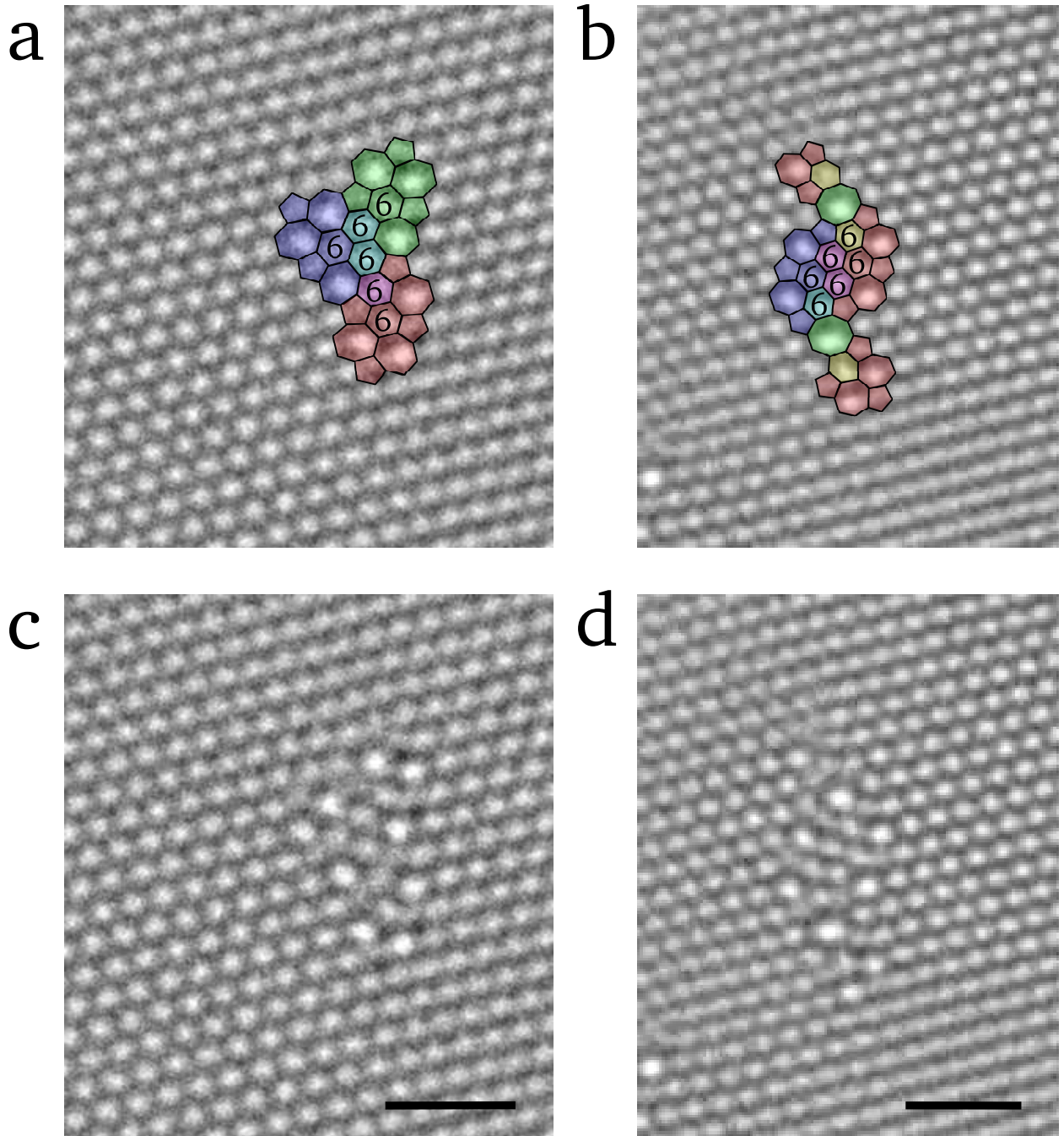


Figure 5: Two examples of defect structures created by short 300 keV exposure and imaged at 80 keV. In the upper row (panels a,b) DFT-optimized configurations are superimposed over the experimental images. Lower row (panels c,d) displays the structures without DFT-overlays. The first structure (a,c) can be constructed by combining three  $V_2(5555-6-7777)$  reconstructed di-vacancies (6 missing atoms), whereas the second one (b,d) can be formed from two  $V_2(5555-6-7777)$ 's, two  $V_2(5-8-5)$ 's, one  $V_2(555-777)$  and one (55-77) defect (total of 10 missing atoms), as indicated by the colors. Scale bars are 1 nm.

shows individual exposures in each frame.

*Supplementary video S4:* A cluster of several vacancy defects, generated by brief 300 keV irradiation and observed at 80 keV. The video shows individual exposures in each frame. The configuration changes continuously until the final, linear aligned di-vancy configuration is observed and stable throughout several exposures (frames 22–29). Frames 30–36 are duplicates of frame 29 in order to show the final configuration as a still image at the end.

*Supplementary video S5:* Generation and transformation of defects under 100 keV irradiation. Each frame is an average of 10 CCD exposures (recorded at a lower current density). This video shows the generation of the rotated hexagon kernel as in Figure 4 of the main article. The rotated hexagon kernel is highlighted as overlay in frames 28–31.

- 
- [1] J. C. Meyer, C. O. Girit, M. F. Crommie, and A. Zettl, *Appl. Phys. Lett.* **92**, 123110 (2008).
  - [2] P. Thévenaz, U. Ruttimann, and M. Unser, *IEEE Transactions on Image Processing* **7**, 27 (1998).